

DISCOVERY OF A LOW SURFACE BRIGHTNESS OBJECT NEAR SEYFERT'S SEXTET

TAKASHI MURAYAMA¹, SHINGO NISHIURA, AND TOHRU NAGAO¹

Astronomical Institute, Graduate School of Science, Tohoku University, Aoba, Sendai 980-8578, Japan;
 murayama@astr.tohoku.ac.jp, nishiura@astr.tohoku.ac.jp, tohru@astr.tohoku.ac.jp

YASUNORI SATO¹

Institute of Space and Astronautical Science, 3-1-1 Yoshinodai, Sagami-hara, Kanagawa 229-8510, Japan;
 sato@astro.isas.ac.jp

YOSHIAKI TANIGUCHI¹

Astronomical Institute, Graduate School of Science, Tohoku University, Aoba, Sendai 980-8578, Japan;
 tani@astr.tohoku.ac.jp

AND

D. B. SANDERS

Institute for Astronomy, University of Hawaii, 2680 Woodlawn Drive, Honolulu, HI 96822;
 sanders@ifa.hawaii.edu

Draft version December 7, 2018

ABSTRACT

We report the discovery of a low surface brightness (LSB) object serendipitously found during deep CCD imaging of a compact group of galaxies, Seyfert's Sextet, in *VR* and *I* bands. The LSB object is located 2'3 southwest from the group center. Its surface brightness within the angular effective radii of $r_e(VR) = 4''.8$ and $r_e(I) = 4''.8$ is very low — $\mu_e(VR) = 25.28$ mag arcsec⁻² and $\mu_e(I) = 24.47$ mag arcsec⁻², respectively. The apparent magnitudes are $m_{AB}(VR) = 19.87$ mag and $m(I) = 19.06$ mag. The object is most likely a LSB dwarf galaxy, but other possibilities are also discussed.

Subject headings: galaxies: dwarf — galaxies: photometry

1. INTRODUCTION

Low surface brightness (LSB) galaxies have been extensively discussed within the context of the overall formation and evolution of galaxies as well as observational cosmology, and in particular for their possible contribution as a major fraction of the total galaxy population (see Impey & Bothun 1997, for a review). During deep imaging observations of the compact group of galaxies known as Seyfert's Sextet (Nishiura et al. 1999) we found a LSB galaxy candidate near the group. In the present paper, we report on the photometric properties of this LSB candidate. We adopt a Hubble constant of $100 h$ km s⁻¹ Mpc⁻¹ throughout this paper.

2. OBSERVATIONS AND DATA REDUCTION

The observations were carried out at the University of Hawaii 2.2m telescope using the 8192×8192 (8k) CCD Mosaic camera (Luppino et al. 1996). The camera was attached at the f/10 Cassegrain focus and provided a $\sim 18' \times 18'$ field of view. The CCDs were read out in the 2×2 pixel binning mode which gave an image scale of $0''.26$ pixel⁻¹. We obtained broad band images with the *VR* and *I* filters on 1999 May 20 and May 23 (UT), respectively. The integration time for each exposure was set to 8 minutes. Twenty-three exposures for the *VR*-band and 24 exposures for the *I*-band were taken, thus the total integration time amounted to 184 minutes in *VR* and 192 minutes in *I*.

Data processing was done in a standard way using IRAF². After bias and dark counts were subtracted, each

frame was divided by the flatfield image, which was a median image of all of the object frames obtained during a night. The object frames were median-combined with their positions registered. Typical seeing, as estimated from the processed images, was $\sim 0''.8$ in both bands. Standard stars from Landolt (1992) were observed and used for calibration of absolute fluxes. Since the *VR* filter is not a standard photometric band (see Jewitt, Luu, & Chen 1996), we adopted an AB magnitude scale for this bandpass. The absolute photometric errors were estimated to be ± 0.05 mag for the *VR*-band and ± 0.03 mag for *I*-band. The limiting surface brightnesses are $\mu_{VR}^{\text{lim}} = 28.7$ mag arcsec⁻² and $\mu_I^{\text{lim}} = 28.1$ mag arcsec⁻², corresponding to a 1σ variation in the background.

3. RESULTS

In Figure 1 we show the *VR*- and *I*-band images of Seyfert's Sextet. A faint, extended object is located in both bands at 2'3 southwest from the group center of Seyfert's Sextet. Our estimate of the centroid position of this faint object is $\alpha(\text{B1950})=15^{\text{h}} 56^{\text{m}} 51''.6$, $\delta(\text{B1950})=+20^\circ 52' 42''$. As shown in the lower panels of Figure 1, the shape of the object appears to be nearly spherical in both bands and very diffuse compared with the foreground/background galaxies around it. There is no evidence that the object moved during the *VR* and *I* observations (the *VR* image was taken three days prior to the *I* band image), thus the object is not likely to be within our solar-system.

Using a wavelet package in ESO-MIDAS,³ we applied

¹Visiting Astronomer of the University of Hawaii 2.2 meter telescope.

²Image Reduction and Analysis Facility (IRAF) is distributed by the National Optical Astronomy Observatories, which are operated by the Association of Universities for Research in Astronomy, Inc., under cooperative agreement with the National Science Foundation.

³European Southern Observatory Munich Image Data Analysis System (ESO-MIDAS) is developed and maintained by the European South-

a Wiener-like wavelet filter to the images in order to improve the signal-to-noise. The results are shown in Figure 2. In the central region of the processed *VR* image there seem to be two intensity peaks lying along a northwest-southeast direction with a separation of $\sim 2''.5$. On the other hand, the *I*-band image shows a single peak which is located between the two *VR* peaks. This could be interpreted as being due to an inhomogeneous distribution of dust, or perhaps a strong emission line from ionized gas that appears in either band. Alternatively, the intensity peaks near the center may be background galaxies. At $19''$ west of the center of the faint object there is another diffuse condensation which could perhaps be interpreted as a tidal structure. This companion structure appears to be present in the original images, but given that the strength of this feature is comparable to the noise uncertainty in the original images, we will not discuss it further in this paper.

Next we discuss the photometric properties of this LSB object. Since the object appears to be nearly spherical, we will adopt a circular aperture for computing the radial light distribution. Apparent foreground/background objects were first masked, and the surface brightness on the original images was then determined using $0''.8$ radial bins where the binwidth was set to be approximately equal to the seeing. The center of the aperture was fixed at the position of the intensity peak in the noise reduced *I*-band image. Figure 3 shows the surface brightness profiles in both bands. These profiles cannot be simply fit with an exponential disk as can be seen by the fact that an exponential profile would appear as a straight line on the μ - r plot (the upper panel of Figure 3). Although the observed radial profiles could be approximated by a straight line fit at radii $4'' \lesssim r \lesssim 10''$, it is clear that the profiles flatten at $r \lesssim 4''$. Furthermore, a $r^{1/4}$ -law profile, which is more centrally concentrated than an exponential profile, is also a poor approximation to the observed data points. We also note that since the flattened region of the profiles is large compared to the seeing size of $\sim 0''.8$, the flat profiles at $r \lesssim 4''$ are a genuine property of this LSB object.

In order to more accurately approximate the observed radial surface brightness distribution, we decided to adopt a $r^{1/n}$ -law fit with $n < 1$;

$$\mu(r) = \mu_0 + 2.5(\log_{10} e) \left(\frac{r}{s} \right)^{1/n},$$

where $\mu(r)$ is the surface brightness at a radius of r from the center, μ_0 is the central surface brightness, and s is the angular scale length. This profile is less concentrated than an exponential profile, i.e., shallower at the inner area and a steeper profile at the outer area than an exponential profile. The solid curves shown in Figure 3 are the best fit for each band. We used only the points at $1'' < r < 10''$ (shown by the filled circles in Figure 3) to avoid the seeing effect at the center and the sky-noise limited area at large radii. Table 1 lists the fit parameters (n , μ_0 , and s) as well as other photometric properties which were subsequently derived. Our analysis shows that the LSB galaxy has a $r^{1/n}$ surface brightness profile with $n \sim 0.6$.

4. DISCUSSION

We first discuss the observed properties of our candidate LSB galaxy in terms of the known properties of LSB galaxies. The color of our LSB candidate is $VR - I \simeq 0.81$. Since the *VR*-band is inconvenient for comparison with standard photometry of galaxies, we first estimated that $V - I \simeq 0.94$ and $R - I \simeq 0.49$ by interpolating the observed fluxes in the *VR*-band and *I*-band. These colors are not peculiar for LSB dwarfs or LSB disk galaxies (e.g., Impey & Bothun 1997). One of the characteristics of our LSB object is the $r^{1/n}$ surface brightness profile with $n \sim 0.6$, however the majority of LSB galaxies exhibit an exponential profile, i.e., $n = 1$ (O’Neil, Bothun, & Cornell 1997). On the other hand, many of the fainter dwarf ellipticals in the Fornax cluster have less concentrated profiles than the exponential (Caldwell & Bothun 1987). Davies et al. 1988 also showed that a significant number of LSB dwarf galaxies in the Fornax cluster show $r^{1/n}$ -law profiles with $n < 1$. Furthermore, O’Neil et al. (1997) showed that 17% of the LSB galaxies in their sample have less concentrated surface brightness profiles than an exponential disk although they did not fit the profiles with the $r^{1/n}$ law but instead used a King model profile.

Caon, Capaccioli, & D’Onofrio (1993) found that the value of n is well correlated with the effective radius (R_e) for spheroidal galaxies ranging from the LSB dwarfs in the sample of Davies et al. (1988) to the giant ellipticals in the Virgo cluster. In this context, the observed exponent of $n \sim 0.6$ for our LSB candidate implies that this object is indeed a good candidate for a LSB dwarf galaxy. As shown in Figure 5 of Caon et al. (1993), the LSB dwarfs with $n < 1$ have R_e in a range between $\simeq 0.13$ kpc and $\simeq 1.3$ kpc. Given the angular effective radius of our LSB galaxy candidate of $r_e = 4''.8$, this would imply a distance somewhere in the range of 5.4 Mpc to 54 Mpc, and a corresponding absolute *I*-band magnitude of between -10 mag and -15 mag, which is comparable to those of dwarf galaxies in the Local Group (Mateo 1998). This would imply that our LSB galaxy candidate would be at the faint end of the luminosity function of LSB galaxies (e.g. Impey & Bothun 1997).

If the LSB galaxy is located at the same distance as Seyfert’s Sextet ($44 h^{-1}$ Mpc), one might conclude that the LSB galaxy may have been formed through possible tidal interactions between the group galaxies. The projected separation of the LSB galaxy from the group center is $\approx 30 h^{-1}$ kpc. The LSB galaxy could travel this distance in 2×10^8 years assuming a projected velocity equal to the radial velocity dispersion (138 km s^{-1}) of the group.

At smaller distances than that of Seyfert’s Sextet, only one galaxy is known within 1° of the LSB candidate. It is also a LSB galaxy, F583-1 (= D584-04: Schombert & Bothun 1988; Schombert et al. 1992; Schombert, Pildis, & Eder 1997). The distance toward F583-1 corresponding to its redshift is $25 h^{-1}$ Mpc. If our LSB galaxy is located at the same distance as F583-1, the apparent separation of $23'$ between F583-1 and the LSB galaxy corresponds to $170 h^{-1}$ kpc.

Another possibility is that the LSB object is located at a much smaller distance. This would imply that the LSB object may be a system more like Galactic globular clusters. In fact, a King model profile with a concentration param-

TABLE 1
RESULTS OF $r^{1/n}$ -LAW FITTING AND PHOTOMETRIC PROPERTIES.^a

	<i>VR</i>	<i>I</i>
Exponent of $r^{1/n}$ law (n)	0.57 ± 0.01	0.65 ± 0.01
Central surface brightness (μ_0) [mag arcsec ⁻²]	24.83 ± 0.02	23.90 ± 0.03
Angular scale length (s) [arcsec]	5.35 ± 0.07	4.84 ± 0.08
Total apparent magnitude (m) [mag]	19.87 ± 0.02	19.06 ± 0.03
Angular effective radius (r_e) [arcsec]	4.81 ± 0.07	4.81 ± 0.08
Effective surface brightness (μ_e) [mag arcsec ⁻²]	25.28 ± 0.02	24.47 ± 0.03

^aErrors quoted in this table are formal errors in the fitting.

eter of ~ 0.7 and a core radius of $\sim 4''.0$ is also a good fit to the present LSB object (Note: we have not shown this fit since it is very similar to that shown in Fig. 3). O’Neil et al. (1997) noted a possibility that some LSB objects well fitted with the King profile that were found in their survey may be Galactic LSB globular clusters. Although the concentration parameter of $c \sim 0.7$ of our LSB object is smaller than those of typical Galactic globular clusters (e.g., Chernoff & Djorgovski 1989), globular clusters in the outer halo of the Galaxy (~ 30 – 100 kpc from the Galactic center) have concentration parameters as small as our LSB object (see, for example, Djorgovski & Meylan 1994). The central surface brightness of the globular clusters in the Galactic halo can be as faint as ~ 24 mag arcsec⁻² in *V*, which is comparable to those of LSB galaxies. The clusters in the Galactic halo have larger core radii of ~ 20 pc than globular clusters at smaller galactocentric radii because of smaller tidal forces at larger distance from the galactic center. If the present LSB object is such a distant globular cluster, it should have a core radius of ~ 20 pc. Thus, the apparent core radius of $r_c \sim 4''.0$ leads to a distance toward the LSB object of ~ 1 Mpc. However if this is the case, stars in the LSB would be resolved spatially in our images. Therefore, this possibility can be rejected.

In summary, we have discovered a LSB object near the compact group of galaxies known as Seyfert’s Sextet. The

LSB object is likely to be one of the following: 1) a field LSB dwarf galaxy at a distance of 5.4–54 Mpc, or 2) a LSB dwarf galaxy at the same distance of Seyfert’s Sextet ($44 h^{-1}$ Mpc). Measurement of the redshift, either by optical spectroscopy or by radio observations of H I gas will be necessary to determine which of these descriptions applies.

The authors are very grateful to the staff of the UH 2.2 m telescope. In particular, we would like to thank Andrew Pickles for his technical support and assistance during the observations. We also thank Richard Wainscoat and Shinki Oyabu for their kind help on photometric calibration, Tadashi Okazaki for kindly providing us his program for calculating King model profiles, and Daisuke Kawata for helpful comments. This work was financially supported in part by Grants-in-Aid for Scientific Research (Nos. 07055044, 10044052, and 10304013) from the Japanese Ministry of Education, Science, Sports, and Culture by the Foundation for Promotion of Astronomy, Japan. TM is thankful for support from a Research Fellowship from the Japan Society for the Promotion of Science for Young Scientists. This research has made use of the NASA/IPAC Extragalactic Database (NED) and the NASA Astrophysics Data System Abstract Service.

REFERENCES

- Caldwell, N., & Bothun, G. D. 1987 AJ, 94, 1126
 Caon, N., Capaccioli, M., & D’Onofrio, M. 1993, MNRAS, 265, 1013
 Chernoff, D. F., & Djorgovski, S. 1989 ApJ, 339, 904
 Davies, J. I., Phillipps, S., Cawson, M. G. M., Disney, M. J., & Kibblewhite, E. J. 1988, MNRAS, 232, 239
 Djorgovski, R., & Meylan, G. 1994 AJ, 108, 1292
 Impey, C., & Bothun, G. 1997, ARA&A, 35, 267
 Jewitt, D., Luu, J., & Chen, J. 1996 AJ, 112, 1225
 King, I. R. 1966, AJ, 71, 64
 Landolt A. U. 1992, AJ, 104, 340
 Luppino, G., Metzger, M., Kaiser, N., Clowe, D., Gioia, I., & Mayazaki, S. 1996, ASP Conf. Ser. 88, Clusters, Lensing, and the Future of the Universe, ed. V. Trimble & A. Reisenegger (San Francisco: ASP), 229
 Mateo, M. L. 1998, ARA&A, 36, 435
 Nishiura, S., Shimada, M., Taniguchi, Y., Murayama, T., Sato, Y., Nagao, T., & Sanders, D. B. 1999, in preparation
 O’Neil, K., Bothun, G. D., & Cornell, M. E. 1997, AJ, 113, 1212
 Schombert, J. M., & Bothun, G. D. 1988, AJ, 95, 1389
 Schombert, J. M., Bothun, G. D., Schneider, S. E., & McGaugh, S. S. 1992, AJ, 103, 1107
 Schombert, S. E., Pildis, R. A., & Eder, J. A. 1997, ApJS, 111, 233

FIG. 1.— The VR - and I -band images of Seyfert's Sextet (upper panels). The newly discovered LSB object is in the center of the box at the lower right.

FIG. 2.— The noise reduced images of the LSB object processed with a Wiener-like wavelet filter. In the lower panels the boxed region is shown at a different intensity scale.

FIG. 3.— The surface brightness profiles of the LSB object in the VR - and I -bands versus the angular radius in linear scale (upper panel) and in logarithmic scale (lower panel). Observed data are shown as filled and open circles with error bars. The filled circles denote the data points which were used for the $r^{1/n}$ -law fit. The results of the $r^{1/n}$ -law fit are shown by the solid lines.

This figure "fig1.gif" is available in "gif" format from:

<http://arxiv.org/ps/astro-ph/0001071v1>

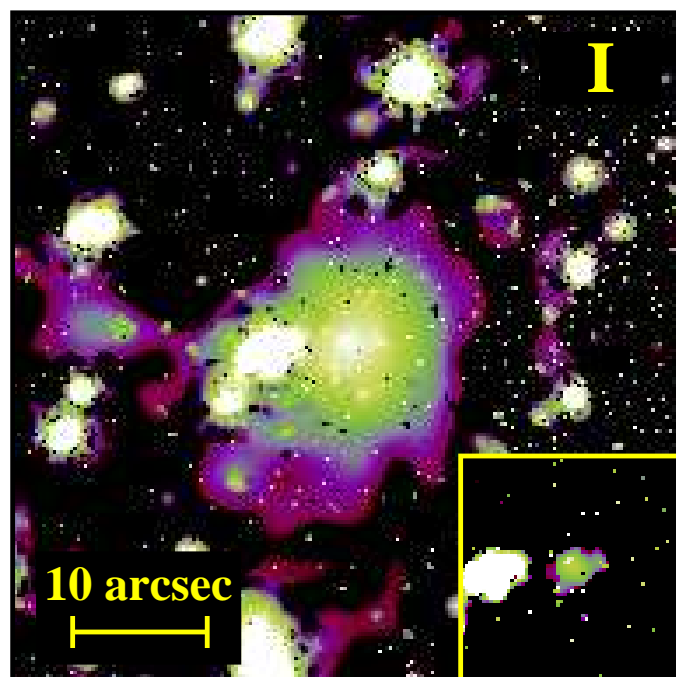
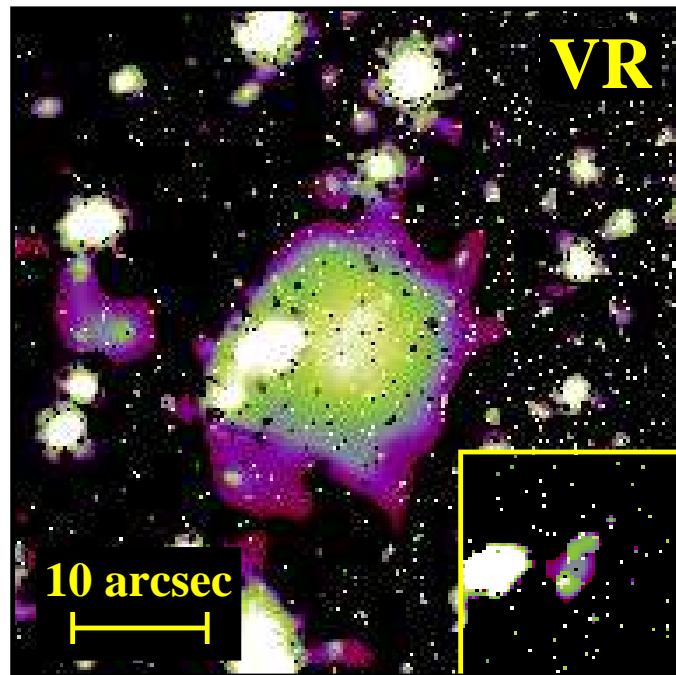


Figure 2

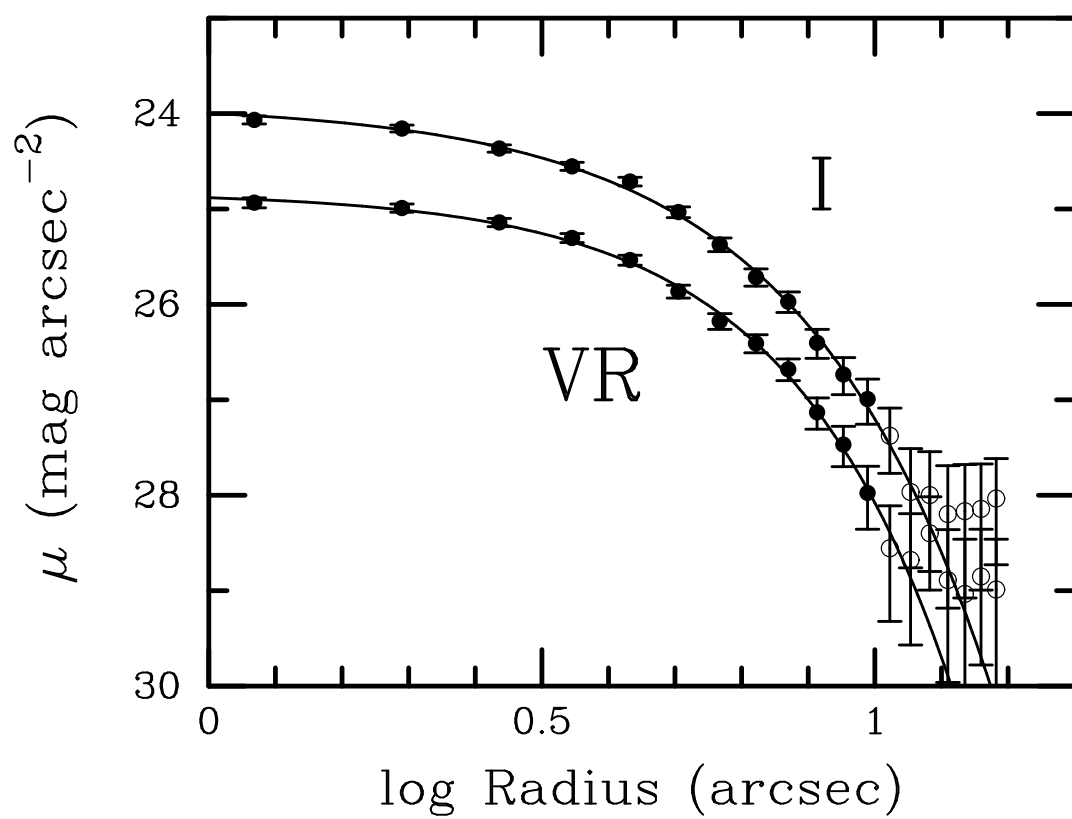
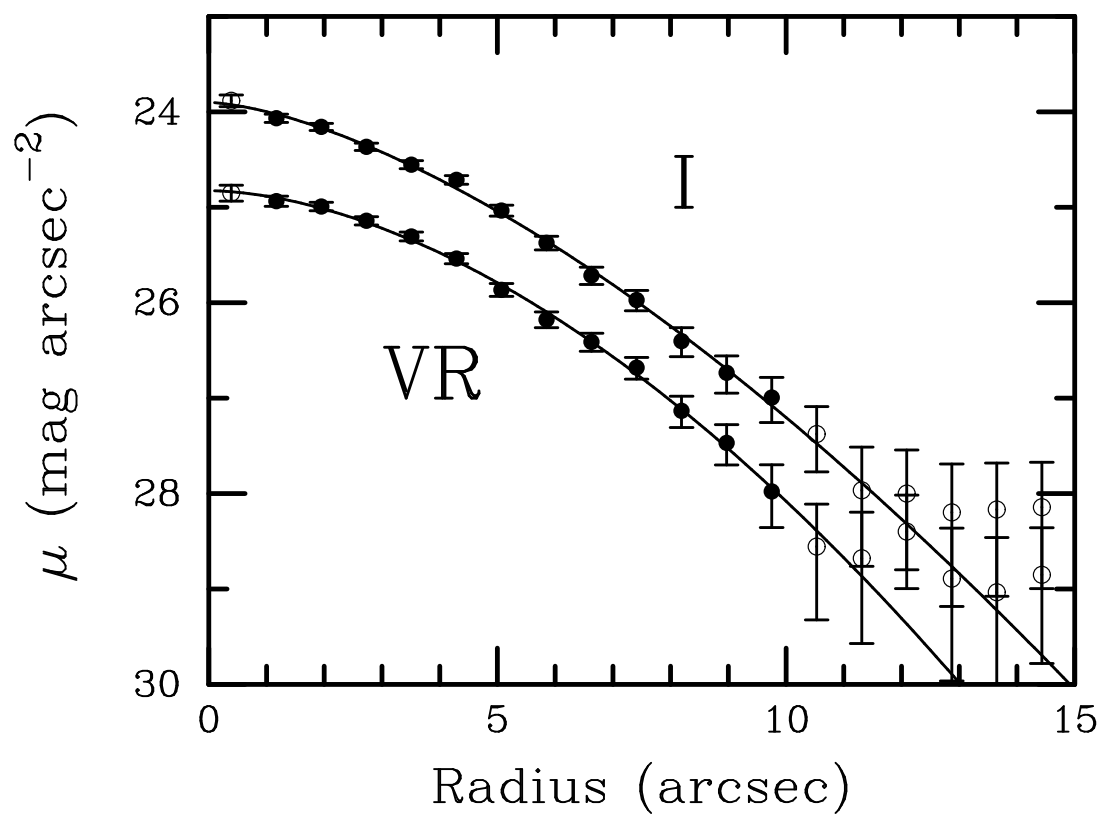


Figure 3